QUALITY ASSURED AIRCRAFT FUSELAGE PRODUCTION: DATA EVALUATION OF A QUALITY CONTROL SENSOR FOR THERMOPLASTIC AUTOMATED FIBER PLACEMENT

M. Mayer, A. Schuster, L. Brandt, D. Deden, F. Fischer, D. Schmorell, M. Vistein
German Aerospace Center (DLR), Center for Lightweight Production Technology (ZLP),
Am Technologiezentrum 4, 86159 Augsburg, Germany

Abstract

In-situ thermoplastic automated fiber placement (TP-AFP) is a lean additive manufacturing process without further vacuum bagging and autoclave cycling. Heated by laser and subsequently compacted with a consolidation roller, the tapes are consolidated on the fly. This makes TP-AFP a single stage manufacturing process. For this highly transient process inline quality assurance (QA) is vital.
The inline QA sensor is situated about 100 mm behind the consolidation roller and measures height profiles via laser triangulation. The evaluation routine identifies gaps and overlaps between tows and tracks as well as early/late cut at the beginning and end of each track. Processing the profile data includes outlier removal, thresholding, bitwise operations, the Sobel operator, erode and dilate operations and contour finding.
We present the data evaluation of a full-scale fuselage skin of a test shell which was produced with a multi-tow laying head that processes three ½" carbon fiber tapes. The primary focus is the detection of gaps and overlaps. A 3D spatial plot will give an overview where the production process has to be revised.

Keywords: thermoplastic composites, LM-PAEK, laser triangulation sensor, inline quality assurance, process monitoring, tape placement sensor, data evaluation, Sobel operator, thermoplastic Automated Fiber Placement, production technology, MFFD, multifunctional fuselage demonstrator

1. INTRODUCTION

The DLR Center for Lightweight Production Technology (ZLP) in Augsburg is part of the European CleanSkyII Large Passenger Aircraft (LPA) program producing the upper shell of the so-called multifunctional fuselage demonstrator (MFFD). Together with the project partners AIRBUS, Aernnova and Premium AEROTEC, the ZLP produced a test demonstrator to verify and adapt the process steps towards the production of the final demonstrator with a length of 8 m and single aisle configuration. First is the in-situ TP-AFP of the fuselage skin by DLR. Followed by the production of compression molded Z-stringers by Aernnova. The DLR integrates these stringers with the technology of continuous ultrasonic welding. The project partner PAG delivers C-frames, which are compression molded tape placed preforms. Finally, the frame integration is done by DLR using resistance welding.

The production data set of in-situ TP-AFP comprises various process parameters that monitor the layup head and the robot, as well as measurement data collected by a quality control sensor. It allows the downstream assembly steps to operate on a fully documented and quality assured skin. This data is important for example to exactly locate ply boundaries and thickness variations underneath welding zones for stringers and flanges. A complete feedback loop from computer aided design (CAD) over offline tape placement programming to the measured component has been established, which allows for detailed analysis of the processing tolerances to the initial design to manufacturing.

With the tape placement sensor (TPS) presented in this work quality can be assured in-line. One of the challenges arising from the single stage TP-AFP process is, that no second process step can repair measured defects. Unlike other CFRP production methods, the TP-AFP process has only one step in which the material transitions into the component. Defects detected in overrun ([7], meaning the measurement system is placed behind the placement process) can only be minimized inline, if they are suitable for a control loop, like gaps and overlaps by adjusting the pressure of the consolidation roller for example. It is also an opportunity to use a trained examiner who can assess whether intervention is necessary after each placed track. The detection of early/late cuts or adds can serve as offset parameter not until the next tape cut. And if anomalies like twists or wrinkled tows are captured in overrun, they can only be used for documentation purposes or, if the specifications allow it, rework. [1] and [7] discuss further types of defects and identify possible detection methods. [9] defines the Airbus specifications for gaps and overlaps.

2. EXPERIMENTAL SETUP

For our experimental setup, the multi-tow layup head (MTLH) by AFPT is mounted to a standard 6-DOF articulated robot on an additional linear axis. Three ½" tapes are deposited in parallel. Commonly each track is placed parallel to the adjacent predecessor track [8]. To measure simultaneously to the layup of tracks, the TPS is mounted on the end-effector. It acquires data of the consolidated tape about 100 mm behind the consolidation roller. The sensor itself is a laser triangulation sensor with high resolution, point density and frame rate. Advanced adjustability for area of interest (AOI), filters and illumination criteria for the height profile generation are available by the

doi: 10.25967/570129

camera hardware. Measurement data consist of height profiles across every placed track and in part neighboring tracks, annotated with the position of the sensor on the workpiece. The height information for one track is stored in a 16 bit TIFF file with additional metadata such as position, trigger coordinates, calibration data stored in separate files. All data is collected in a database for further analysis.

3. INLINE QA SENSOR

The inline QA sensor is mounted on the layup head to record the height profiles after the tapes have been consolidated (FIG 1). Since carbon fibers tend to reflect incident light in total reflection, a 90° angle between line laser plane and camera with 45° between camera and surface turned out to be optimal to get the maximum light output.

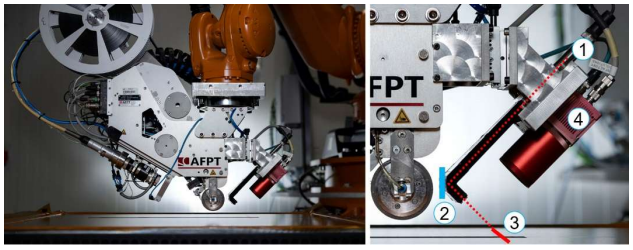

FIG 1. Left: Multi-tow laying head with mounted inline QA sensor on the right side. Right: Close up of inline QA sensor. 1) Source of line laser. 2) Mirror. 3) Laser line on tape surface. 4) Camera for laser line detection.

A mirror is used to make the system more compact. The laser is a Class 3B 660 nm line laser. The camera has a sensor matrix size of 2048 x 2048 pixels. There are different algorithms which evaluate the sensor matrix onboard and deliver chunks of profiles to the user. To speed up the onboard evaluation, an area of interest (AOI) can be defined. The AOI is adjusted dynamically to prevent the laser line from wandering out of the AOI. The inline data evaluation of the delivered height profiles is then also carried out in a chunk-based mode, which allows neighboring pixels of the preceding and following height profile to be taken into account, as opposed to evaluating only a single height profile. With the evaluation pipeline presented in this paper a minimum chunk size of 100 lines is necessary.

FIG 2. Left: TPS. Right: Height profiles of one track stored in a 16 bit tif file. Numbers for both images: 1) Left tow. 2) Middle tow. 3) Right tow. 4) Layup direction.

The TPS is triggered by an encoder interface which is emulated by the robot controller. For each encoder pulse, a height profile line is created. Triggering is set to a position distance of 0.4 mm. FIG 2 depicts the recording process. The 16 bit image on the right represents one track and is the basis for the data evaluation pipeline. The data was collected during the production of a demonstrator part as shown in FIG 3, which consists of hundreds of tracks with different lengths.

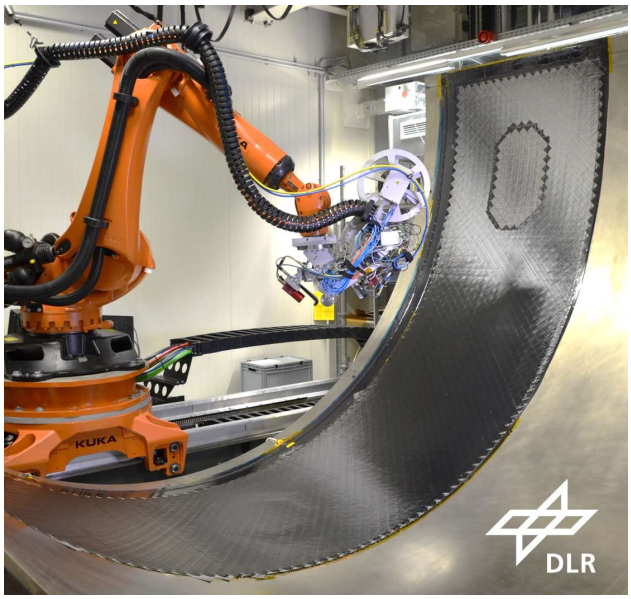

FIG 3. test shell

4. CALIBRATION

The Tool Center Point (TCP) of the tape laying process is located directly at the consolidation roller. Its coordinates are transferred by the robot controller to the measurement system in real-time every 0.4 mm. In the first calibration step, the coordinate transformation between the TCP and the internal coordinate system of the TPS must be determined to allow the interpretation of measured data in workpiece coordinates. For this purpose, a helper base is measured and the sensor is aligned with it (FIG 4 3)).

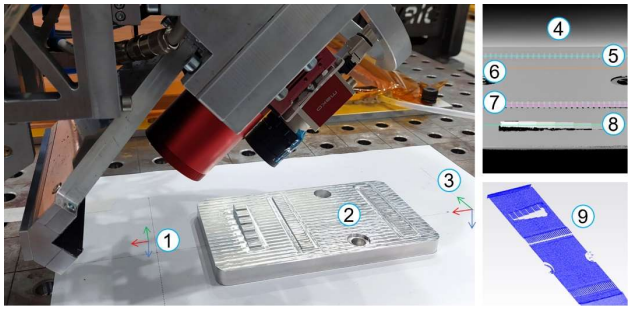

FIG 4. Left: TPS and calibration target. Right top: image with profiles of calibration target and hand-marked features. Right bottom: Point cloud of calibration target. Numbers: 1) TPS TCP. 2) Calibration target. 3) Helper base. 4) Height-image of calibration target. 5) and 7) Features to calibrate the Y coordinate. 6) and 8) Features to calibrate the Z coordinate. 9) Point cloud.

The TPS coordinate system is oriented with the X-axis points in direction of the layup motion and the Z-axis is normal to the workpiece surface. Due to the 45° angle between the laser-light plane and the surface, measured deviations of the laser line are not only affecting the Z coordinate, but also the X and (to a much smaller extend) the Y coordinates. A precisely manufactured, standardized calibration target, with a surface roughness of Rz 10, is used to perform this calibration step.

It features a number of defined structures that allow the determination of all necessary offsets. The calculations include a detrending of the laser line by using the flat surface of the calibration target in FIG 4 6) and enable the correlation between height information and grey values with the help of steps shown in FIG 4 8). Furthermore, the Y resolution depending on the height can be measured by the rectangle shaped features 5) and 7) in FIG 4. After both calibration steps have been completed, each pixel in the height-map received from the sensor can be located in 3D coordinates of the workpiece.

This procedure allows a quick, recurring check of the system functionality necessary to avoid optical misalignment, which may lead to a reduced resolution. This is especially true for gaps [2]. A daily or even more frequent check is advisable.

Actual parameters for the sensor:

Resolution:

X-direction: 0.400 mm (encoder resolution, layup direction)
Y-direction: 0.041 mm/pixel (along the laser line)
Z-direction: 0.027 mm/pixel (normal to the surface)

Measurement range:

X-direction: track length
Y-direction: 84 mm
Z-direction: 37 mm

5. DATA EVALUATION

Our approach is based on a lightweight computer vision algorithm. Another approach based on machine learning has been described in [6]. Compared to [6] we focus on an implementation in C++ with the OpenCV framework. Our application is specialized to find overlaps and gaps and also shows potential to find early/late adds and cuts. Its validated on a skin of a fuselage test shell comprising 98 plies, some of them cover the whole component others are smaller patches. FIG 3 provides a size ratio of the manufactured part.

For deeper analysis and algorithm refinement, the data is processed offline, but measurements of execution time indicate the possibility for real-time usage. At the beginning, we focused on a profile-based approach, i.e. using only one height profile at a time to detect overlaps and gaps [2][3]. This method is very susceptible to noise and interference in the data as there is no information on adjacent height profiles. This leads to many false positives. To include neighboring information, a kernel-based procedure was considered. This approach provides less false positives and a qualitatively good result.

The kernel-based processing is visualized in FIG 5. The height profile image is split up into multiple kernels. Because three tapes are used, four tow-borders can be expected. For each tow-border, a kernel with a height of 200 lines is created. The next kernel for each tow-border is displaced by 100 lines, therefore overlapping with the previous one. While the following processing steps are performed on each whole kernel, only the central 100 lines are later used for classification of gaps, overlaps, rising or falling edges. This allows to avoid artefacts that can occur at the borders of kernels, by still covering the whole track (minus the first and last 50 lines which are out of the manufactured part). By using a kernel-based evaluation, edge detection and other processing steps provide a much more reliable result.

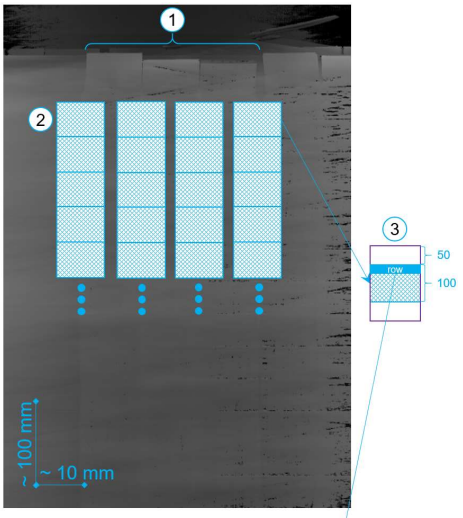

4

	row	towborder0	towborder1	towborder2	towborder3	position
kernel0	0	g	n	o	f	xyzabc
	1	n	n	o	f	xyzabc
	2	r	n	n	g	xyzabc
	...	...	...	...	...	xyzabc
	99	g	n	o	f	xyzabc
kernel1	100	g	n	o	f	xyzabc
	101	n	n	o	f	xyzabc
	102	r	n	n	g	xyzabc
	...	...	...	...	...	xyzabc
	199	g	n	o	f	xyzabc
kernel2	200	g	n	o	f	xyzabc
	201	n	n	o	f	xyzabc
	202	r	n	n	g	xyzabc
	...	...	...	...	...	xyzabc
	299	g	n	o	f	xyzabc

etc.

FIG 5. 1) One track, the predecessor track is on the right. Each row in the tif represents one height profile. 2) 100 rows in the middle of a kernel. Every towborder has its own kernel. 3) Kernel with 200 rows. 4) One row in the kernel provides a result (n, g, o, r, f) for one towborder

A simplification of the evaluation pipeline for one kernel is visualized in FIG 6 that shows a gap between 2 tows. The first step removes outliers by combining thresholding, mean and standard deviation calculations as well as masking and median blur application (FIG 6 2)). Next is the usage of the Sobel operator in horizontal direction to detect the edges (FIG 6 3)) [4][5]. The following thresholding highlights the edges but also some noise (FIG 6 4)). The erode function is used to separate the noise fragments (FIG 6 5)). The first contour finding function just eliminates those fragments (FIG 6 6)). The left highlighted edges are then dilated,

because now it is useful to melt fragments together (FIG 6 7)) in contrast to the previous step. Now the final contour finding function is applied (FIG 6 8)): Contours that exceed the defined aspect ratio are discarded as well as contours that deviate more than +/- 45 degrees from the vertical. The contour is also discarded, if it is too close to the left or right border of the kernel. The detected contours are then used as a mask (FIG 6 8)) to combine the Sobel values with the mean value of the Sobel matrix serving as background (FIG 6 9)). Now the central 100 lines of the kernel are ready for row-based evaluation (FIG 6 10)).

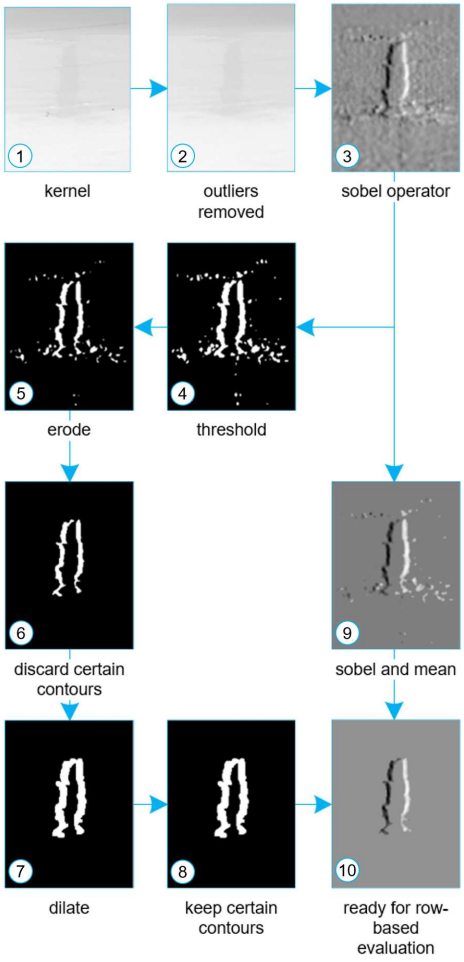

FIG 6. Simplified data evaluation pipeline for one kernel showing a gap between two tows

Stepping through one row from left to right, a falling edge can be detected if the value is lower than the mean, and a rising edge, if its higher. Gaps and overlaps each consist of 2 edges, depending on the first occurrence of rising or falling. A single detected edge can be a rising or falling edge, i.e. if the neighboring track was not placed yet or the tapes are missing. All other cases are not considered and treated as nominal (n).

6. RESULTS

In FIG 7 an example image is overlaid with the results, where green stands for single rising, yellow for single falling edge, blue for a gap and red for an overlap, nominal results are not displayed. In the figure the previous track is on the right, so the left edge must be a rising edge. There are a few false detections on the fourth tow-border in the bottom, but most detections are correct in a visual comparison to the original image.

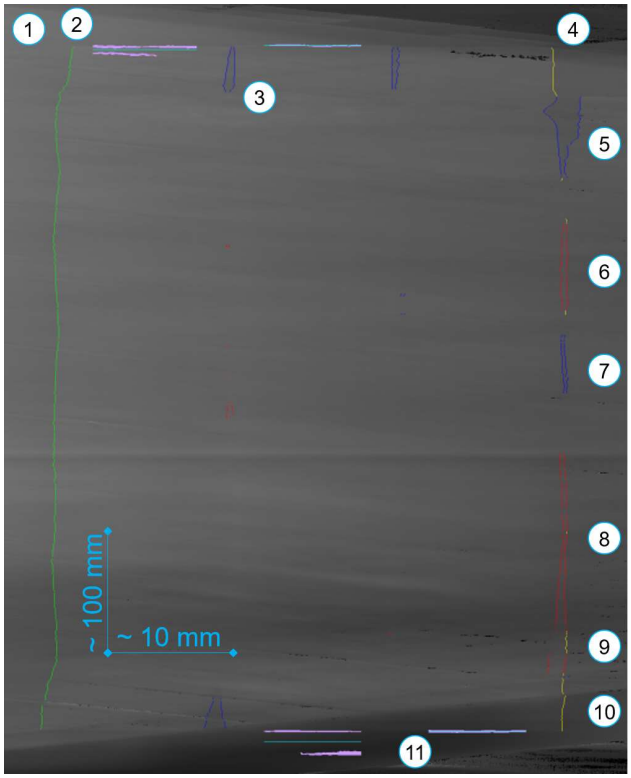

FIG 7. 1) Image overlaid with results. 2) First towborder, which only can be a rising edge. 3) Gap between two tows. 4) Detections between actual track and its predecessor. 5) and 7) Correct gap detections. 6) and 8) Correct overlap detections. 9) Incorrect falling edge detections. 10) Correct falling edge detection, because predecessor track is shorter. 11) Tape end detection

A plot of all gaps between the tracks of one ply covering the whole part is shown in FIG 8. If the gap is smaller than 0.5 mm, it is displayed in green. Yellow between 0.5 to 1.5 mm, red for gaps of 1.5 to 2.5 mm, black for gaps above 2.5 mm. After mechanical corrections on the MTLH in the center of the ply, an increase in the size of the gaps can be seen in some tracks. In addition, gaps of 0.5 to 1.5 mm are visible in the right corner to a certain extent, the cause of which is unknown.

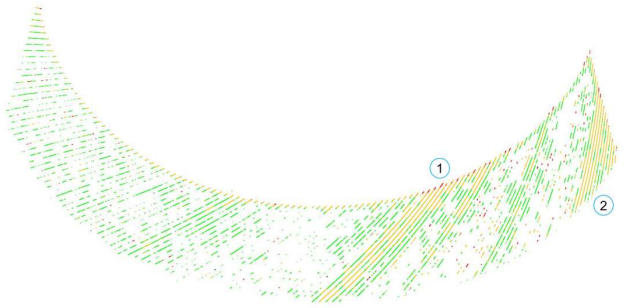

FIG 8. Visualization of gaps between the track of one ply covering the whole part. 1) and 2) Cluster of gaps of 0.5 to 1.5 mm

The visualization is done with the open source point cloud library (pcl). Overlaps and/or rising/falling edges can also be displayed.

The automated evaluation has been validated by a plate with specific gaps and also manual measurement. The order of the magnitude of the deviations provided by the evaluation algorithm is ±0.5 mm accurate at the verified points.

7. CONCLUSION

The developed lightweight OpenCV pipeline, using C++ as programming language, offers a sufficiently fast way to detect gaps and overlaps. The evaluation of a kernel takes an average of 13 ms. With the current parameters and the setup with overlapping kernels, 100 height profiles can be evaluated for every 40 mm (or 320 ms) during tape laying with constant speed of 125 mm/s, which can enable inline feedback. The plies of the demonstrator part that have been evaluated show a good detection quality.

8. OUTLOOK

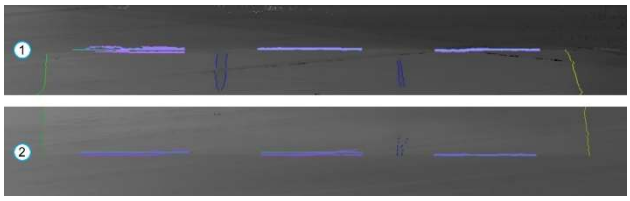

FIG 9. 1) Detection of the track begin for each tow. 2) Detection of the track end for each tow.

The evaluation pipeline was adapted to detect early/late adds or cuts by using the Sobel operator in vertical direction. The contour is filtered by different criteria. FIG 9 demonstrates the correct location of the tape begin and end. For every track the target position is stored to determine the deviation of the tape begin and end. One drawback is that the detection of early/late adds or cuts still has too many false negatives or is not located correctly, as shown in previous FIG 7. However, it seems worthwhile to perform further optimizations of the pipeline.

The evaluation pipeline presented in this paper could likely be improved with regard to the false negative rate by adjusting the parameters of the different pipeline steps. The pipeline itself is fast, but there is a high potential for optimizing the output rate of the sensor hardware by reducing the AOI and therefore increasing the profile rate. In combination with a higher resolution of the encoder providing the coordinates of the measurement, the resolution could be improved.

By organizing the data in a spatial database, a 3D visualization revealing the defect location and clustering would be much more effective and useful for the user than just plotting data for one ply as presented in this paper.

9. ACKNOWLEDGEMENTS

This project has received funding from the Clean Aviation Joint Undertaking (CAJU) under grant agreement CS2-LPA-GAM-2020-2023-01. The JU receives support from the European Union's Horizon 2020 research and innovation programme.

10. DISCLAIMER

The results, opinions, conclusions, etc. presented in this work are those of the author(s) only and do not necessarily represent the position of the CAJU; the CAJU is not responsible for any use made of the information contained herein.

REFERENCES

[1] E. Oromiehie, B. G. Prusty, P. Compston und G. Rajan, „Automated fibre placement based composite structures: Review on the defects, impacts and inspections techniques," Composite Structures, Volume 224, 2019.

[2] A. Schuster, M. Mayer, L. Brandt, D. Deden, F. Krebs und M. Kupke, „Inline Quality Control for Thermoplastic Automated Fiber Placement by 3D Profilometry," in *SAMPE Europe*, Switzerland, 2021.

[3] A. Schuster, M. Mayer, M. Willmeroth, L. Brandt und M. Kupke, „Inline Quality Control for Thermoplastic Automated Fibre Placement," in *30th International Conference on Flexible Automation and Intelligent Manufacturing (FAIM2021)*, Greece, 2021.

[4] G. Bradski und A. Kaehler, Learning OpenCV: Computer Vision with the OpenCV Library, O'Reilly Media, Inc., 2008.

[5] „https://docs.opencv.org/4.5.5/," [Online]. Available: https://docs.opencv.org/4.5.5/d2/d2c/tutorial_sobel_derivatives.html. [accessed on 12 09 2022].

[6] S. Meister, „Automated Defect Analysis using Optical Sensing and Explainable Artificial Intelligence," Delft University of Technology, 2022.

[7] K. Schlegel, P. Parlevliet, C. Weimer, A. Schuster und M. Kupke, „A literature review of quality control," *Journal of Plastics Technology 15,* 2019.

[8] D. Deden, L. Brandt, O. Hellbach und F. Fischer, „UPSCALING OF IN-SITU AUTOMATED FIBER PLACEMENT WITH LM-PAEK - FROM PANEL TO FUSELAGE," European Conference on Composite Materials, Switzerland, 2022.

[9] „AIPS 03 02 019, Issue 11," Airbus S.A.S., Engineering Directorate, 31707 Blagnac Cedex, Francee, June 2016.